Swabir SILAYI

M.S. Thesis in Physics

June - 2011

INVESTIGATION OF COLLAGEN TYPE II MECHANICAL AND STRUCTURAL PROPERTIES WITH THE ATOMIC FORCE MICROSCOPE

by

Swabir SILAYI

June 2011

INVESTIGATION OF COLLAGEN TYPE II MECHANICAL AND STRUCTURAL PROPERTIES WITH THE ATOMIC FORCE MICROSCOPE

by

Swabir Silayi

A thesis submitted to

The Graduate Institute of Sciences and Engineering

of

Fatih University

in partial fulfillment of the requirements for the degree of

Master of Science

in

Physics

June 2011

Istanbul, Turkey

APPROVAL PAGE

I certify that this thesis satisfies all the requirements as a thesis for the degree of Master of Science.

Prof. Dr. Mustafa KUMRU
Head of Department

This is to certify that I have read this thesis and that in my opinion it is fully adequate, in scope and quality, as a thesis for the degree of Master of Science.

Assoc. Prof. Kurtuluş Gölcük
Supervisor

Examining Committee Members

Assoc. Prof. Kurtuluş GÖLCÜK _____

Assoc. Prof. Levent SARI _____

Assist. Prof. Mustafa Fatih ABASIYANIK _____

It is approved that this thesis has been written in compliance with the formatting rules laid down by the Graduate Institute of Sciences and Engineering.

Assoc. Prof. Nurullah ARSLAN
Director

Date

June 2011

INVESTIGATION OF COLLAGEN TYPE II NANOMECHANICAL AND STRUCTURAL PROPERTIES WITH THE ATOMIC FORCE MICROSCOPE

Swabir SILAYI

M. S. Thesis - Physics

June 2011

Supervisor: Assoc. Prof. Kurtuluş GÖLCÜK

ABSTRACT

Collagens and the networks and matrices they form in the articular cartilage function to provide structural and mechanical support to connective tissue. They resist the tension and also augment the pore fluid pressures within the joints. Knowledge of the biomechanical and structural properties of the collagen molecules is essential in understanding the self assembly of the collagens, the interactions of cells with the extracellular matrices and the relationship between the structures and the biomechanical functions and properties of tissues in addition to discerning the origin and effects of tissue degeneration.

In this study, we used the AFM to examine the mechanical and structural properties of the Collagen Type II protein. The collagens were extracted from bovine cartilage and incubated at room temperature, 23^{o}C, for different periods at different pH values and the effects of these observed from the AFM images. Additionally, single molecule force spectroscopy (SMFS) was done to determine some mechanical properties of the collagen.

The AFM images taken of the collagens at different pH (4, 6, 8 and 10) showed consistency with observations that had been made earlier in literature. Basically, the structure of the collagens changed depending on the pH, with aggregated granules presenting at lower pH 4 and the fibrils becoming more distinct and isolated as the pH increased. Increasing incubation time served to emphasize the fibril formation. The force curves obtained from the SMFS measurements were fitted using the WLC model to give us values of approximately 209nm contour length and 11.72nm persistence length, both comparable to values observed in literature.

Keywords: Collagen Type II; Atomic Force Microscopy, Force Spectroscopy, Worm Like Chain Model.

TİP II KOLLOJENİN YAPISAL VE NANOMEKANİKSEL ÖZELLİKLERİNİN ATOMİK KUVVET MİKROSKOBU İLE İNCELENMESİ

Swabir Silayi

Yüksek Lisans Tezi – Fizik Bölümü

Haziran 2011

Tez Danışmanı: Doç. Dr. Kurtuluş GÖLCÜK

ÖZ

Artiküler katilajı oluşturan kollajenler, ağlar ve matrisler, dokuya yapısal ve mekaniksel fonksiyon sağlarlar. Gerinime ve eklemler arasındaki sıvı basıncına karşı dayanıklıdırlar. Kollajen molekülünün biyomekaniksel ve yapısal özelliklerinin bilinmesi; kollojenlerin oluşumu, hücre dışı matrislerle hücrelerin etkileşimi ve doku dejenerasyonun özünün anlaşılması için önemlidir.

Bu çalışmada, Kollajen Tip II proteinin mekaniksel ve yapısal özellikleri Atomik Kuvvet Mikroskobu (AFM) kullanılarak incelenmiştir. Bovin kartilajından izole edilen Kollajenler oda sıcaklığında farklı pH değerlerde farklı zaman aralıklarında inkübe edilerek etkileri AFM ile incelenmiştir. Ayrıca, tek molekül kuvvet spektroskopisi (SMFS) ile kollajenin mekanik özellikleri incelenmiştir.

Farklı pH (4, 6, 8 ve 10) değerlerinde kollajenin yapısal değişikliklere maruz kaldığı görülmüştür. Düşük pH değerlerde (pH 4) kollajen mollekülleri bir araya gelerek granül yapılarda oldukları gözlenmiştir. Yüksek pH değerlerinde fibril yapılarda oldukları gözlenmiştir. Uzun süreli inkübasyonda fibril oluşumlarının arttığı gözlenmiştir. SMFS ölçümleri WLC modeliyle örtüştürülerek, kontur uzunluğunu 209 nm ve persistans uzunluğu 11.72 nm olarak ölçülmüştür.

Anahtar kelimeler: Kollajen tip II, Atomik Kuvvet Mikroskobu, Kuvvet Spektroskopi, WLC modeli.

To my friends, because I remember

ACKNOWLEDGEMENTS

First and foremost, my sincerest gratitude to Assoc. Prof. Kurtuluş Gölcük for the opportunity that led to this point. I shall be forever grateful for his academic guidance and insight throughout my thesis research, his patience and his confidence in my abilities especially during the first weeks as I tried to find my way around the labs.

I would also like to thank the head of the department Prof. Dr. Mustafa Kumru for his support as I undertook my studies and research. I am thankful also to Assoc. Prof. Bayram Ünal, Assoc. Prof. Levnt Sari, and Assist. Prof. Fatih Abasıyanık for their input and encouragement. For his insights into the finer workings of the AFM, I would also like to thank Assist. Prof. Burak Yılmaz.

From the Biology Department, I thank Res. Asst. Cemile Ümran Ceylan for help and time with the preparation of the biological samples. I am grateful also to Res. Asst. Umidahan Djakbarova of the Genetics and Bioengineering Department for her assistance. Thank you too to all my colleagues and friends in the Physics department. Your company throughout this period really helped make the days that much brighter. To all my family and friends, my gratitude and appreciation for your understanding, motivation and patience.

The financial support for this project was provided by Fatih University under BAP Project # P50011002

TABLE OF CONTENTS

LIST OF TABLES

LIST OF FIGURES

LIST OF SYMBOLS AND ABBREVIATIONS

AFM	: Atomic Force Microscope
$PSPD$	: Position sensitive photo detector
$SMFS$	: Single Molecule Force Spectroscopy
WLC	: Worm Like Chain Model
FJC	: Freely Jointed Chain Model
L_p	: Persistence Length
L_c	: Contour Length
z	: Extension
F	: Applied force
k_B	: Boltzmann constant
T	: Absolute temperature
OA	: Osteoarthritis

CHAPTER 1

INTRODUCTION

Knowledge of the biomechanical and structural properties of collagen molecules is essential to understanding the self assembly of the collagens, the interactions of cells with the extracellular matrices and the relationship between the structures and the biomechanical functions and properties of tissues. Articular cartilage is made up of a meshwork of collagen fibrils and works to augment the fluid pressure within the joint mechanics. As such, we can say that the physiological functions and properties of the cartilage depend on a specific interaction of the molecules that build up its extracellular matrix (ECM). Specifically, it consists mainly of proteoglycans embedded in a fibrillar network of collagens (types II, IX and XI), with Collagen Type II making up almost 80% of cartilage concentration. Together, the collagens and proteoglycans create a hydrated tissue that resists compressive loads within the joints (Shirazi, 2008).

The quality of the articular cartilage and its mechanical properties can be affected by any changes in the composition or structure of the collagens and proteoglycans, and these changes may lead to osteoarthritic (OA) degradation. OA is an age related condition, affecting mostly the elderly and manifests as a degradation of the matrix structure of the articular cartilage. The degradation process starts with a depletion of the proteoglycan gel followed by collagen degradation which leads to mechanical and physical erosion of the macro-structural cartilage itself (Stoltz, 2005). As things stand, OA degeneration can only be diagnosed when the underlying changes in the proteoglycans and collagen matrix have advanced to such a stage as to present as macroscopic damage of the cartilage.

To be able to better manage the degeneration of the cartilage, early detection is of paramount importance. Understanding the structure of the collagens that mesh up to form the cartilage and their biomechanical properties would therefore enable early detection of the onset and management of the OA degeneration before it presents at the macro-level.

The fibrillar collagen itself takes the form of a triple helix formed from a chain of three polypeptides. Rich and Crick have shown that the molecule has a rigid rod structure of approximately 300nm height and radius 1.5 nm (Rich, 1955). In spite of the many studies carried out on the protein, there is still no clear understanding as far as its mechanical properties like hardness or deformation behavior under loads are concerned. Most recently, the protein fibril biomechanical properties have been examined at the nano level through X-ray Diffraction methods and Optical Tweezers and increasingly, with the Atomic Force Microscope (AFM).

Beuhler and Bustamante evaluated its nanomechanical properties theoretically using the Worm Like Chain Model (WLC) at the molecular level (Beuhler, 2006; Bustamante, 1994). Rich, Sun and Ark used Optical Tweezers to show that the Collagen II molecules structure is easily bendable in spite of its rigid structure (Evans, 1997). In addition, they reacted the Collagen II with metalloproteinase and using the AFM investigated the linking and breaking regions of the collagen.

Adachi and Ark also using the AFM examined and showed the difference between normal and mutated Collagen II molecules (Sun, 2004). From their works, Stoltz and Ark applied nano-indentation methods to study the biomechanical properties and the age related morphological changes that present in cartilage, proposing this as an early diagnostic tool for the detection of OA (Adachi, 1999; Stoltz, 2003; Stoltz, 2004).

In this study, we used the AFM to characterize the nanomechanical and structural properties of single molecules of extracted Collagen Type II proteins and the effect of these on the quality of the articular cartilage. The Collagen molecules were immobilized onto a freshly cleaved mica substrate via the carboxyl group and, by applying Single Molecule Force Spectroscopy (SMFS) using the tip of the AFM, the molecule was stretched in solution.

The experimental force-extension curves resulting were fit and analyzed using the WLC. From the results, information on the molecule's nanomechanical properties such as stiffness, persistence length and elasticity was obtained. Additionally, we obtained structural information of the Collagen Type II proteins such as contour length, fibril diameter, D-banding patterns and other information from the AFM images.

Apart from the mechanical and structural properties, we also used the AFM to image and observe the fibril formation behavior of the Collagen Type II under different physiological conditions. By changing the pH of the buffer solution and for different incubation times, we were able to note the differences in fibril formation patterns for each case.

CHAPTER 2

MATERIALS AND METHODS

2.1 Collagens

2.1.1 Collagens to Cartilage

Articular cartilage is made up of a network of collagen fibrils and these work to resist the tensile stresses and strains and also augment the fluid pressure at higher loads of joint mechanics. Depending on their relative positioning within the general structural make-up of the cartilage, the collagen fibrils are oriented differently (see Figure 2.1). Starting from regions closer to the surface, they are horizontally oriented, parallel to the surface. Lower down, in the middle transitional region, they assume a random orientation before finally arranging themselves in a perpendicular (vertical) direction to the lower bone cartilage interface (Shirazi, 2008).

These specific orientations of the collagens far from being random, serve to maintain the integrity and stability of the cartilage structure in its functions. Any damage to or varying of these ultimately exposes the cartilage to possible degenerative changes that may lead to cases of joint failure or even OA. Primarily, the cartilage content consists of almost 80% Collagen Type II (it also includes types IX and XI and other non-collagenous proteins like proteoglycans), so understanding them and their characteristic behavior under stress and strain is key to understanding the workings of the cartilage itself (Gelse, 2003) .

2.1.2 Collagen Structure Overview

Collagens are the major structural component of all connective tissues and can also be found in other tissues and organs. They work to contribute to and maintain structural integrity and stability in the tissues and organs and as such, they have been

greatly studied and especially in recent years, a lot of information has been accumulated on them.

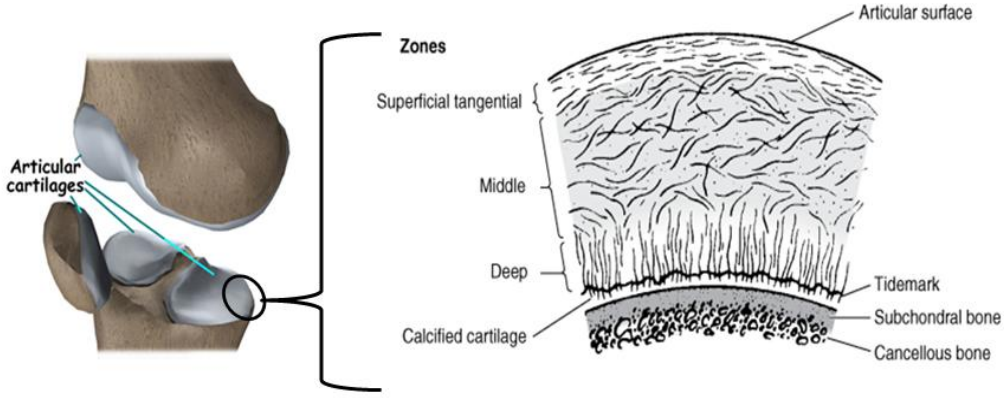

Figure 2.1 Showing articular cartilage and collagen orientation within the different zones of cartilage

All members of the collagen protein family are made up of the domain repeating polypeptide Gly-X-Y, with glycine being the most abundant amino acid. These are the basic building blocks for the triplehelical structure of the collagens, i.e. three polypeptide chains form a characteristic right handed triple helix that is common to all collagens. In the case of Collagen Type II, the three chains are identical (termed homotrimeric). The triple helix in its case is composed of three α1(II)-chains that form a homotrimeric molecule.

The α chains twist around a central axis in such a way as to allow close packaging of the molecule around the axis. The glycines are usually positioned at the center of the helix and with the X and Y positions taken up either by proline or hyroxyproline. This Gly-X-Y helix is the repeating unit that results in a fibril of about 300 nm length and 1.5 nm diameter (Graham, 2005; Rich, 1955).

From the triple helical monomer, micro-fibrils arise. These come about as a result of the monomers arranging themselves in a staggered fashion and they go on to form sub-fibrils which in turn assemble into the fibrils dimensions. The staggered arrangement of the monomers is what is responsible for the D-banding pattern that is observed in the collagen fibrils. From studies (Jiang, 2004), the formation of these D-banding patterns and generally the formation of the fibrils with the resulting structural characteristics under physiological conditions is dependent on both the level of acidity and temperature at which the reconstituting collagens fibrils are kept. Figure 2.2 illustrates the breakdown of the collagen structure.

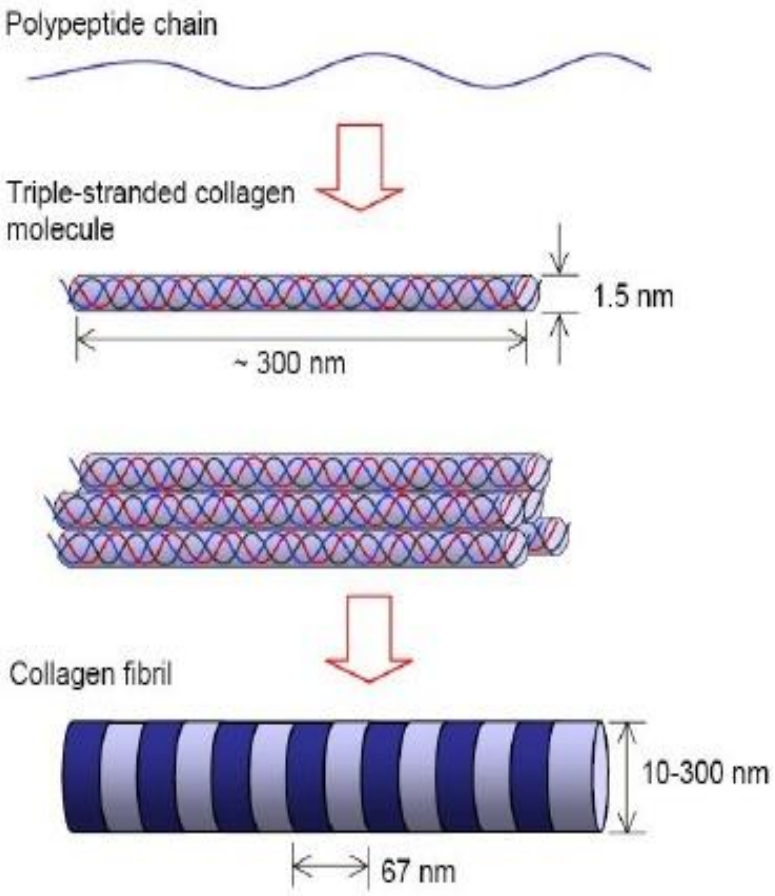

Figure 2.2 Schematic of the assembly of collagenous tissues. Collagen monomers are formed from intertwining polypeptides and they arrange themselves into micro-fibrils then sub-fibrils and the fibrils. This assembly eventually comes to the formation of tissues.

2.2 Atomic Force Microscopy (AFM)

2.2.1 Introduction to the AFM

The AFM, a member of the scanning probe microscope family, was first developed in 1985 by Binnig, Quate and Gerber (Graham, 2005; Zlatanova, 2000), as an enhancement on the Scanning Tunneling Microscope (STM), which had been developed earlier by Binning and Rohrer (Morris, 2010). The development of these made it possible to image at resolutions that had been possible before only with electron microscopy and also allowed imaging of samples in their natural conditions, which had been the reserve of the optical microscopes. This ability to image samples, especially biological, without having to make any modifications to them and to be able to do so at molecular or even higher levels of resolution have made these probes indispensible as far as investigation of (biological) samples go.

With improvements over time, the AFM probes have moved from being used for just imaging samples to becoming tools for a more generalized investigation of other properties of the samples like stiffness, hardness, elasticity, charge distribution, magnetic characteristics and have applications even in surface modification methods like nanolithography. Especially for biological samples, the fact that the AFM can measure molecular forces means that it is used more for the other applications than its original intended purpose of imaging. As in this study, although we imaged the collagen samples using the AFM, primarily, we applied it in the characterization of the single molecules to determine their mechanical properties.

2.2.2 Parts of the AFM

Although it is called a microscope, the AFM has no lens as is the case for conventional optical microscopes. Instead, it works on the principle of a sharp tip affixed onto a cantilever whose oscillations due to force interactions with the sample surface are what give rise to the final image. The very first probes were made from diamond fragments glued onto gold foil (Ricci, 2004). Today they are made mainly from silicon nitride (Si_3N_4) which has a lower mass and force constant with relatively higher resonance frequencies and this allows for a general uniformity for all cantilevers and a high reproducibility of results (Graham, 2005; Ricci, 2004).

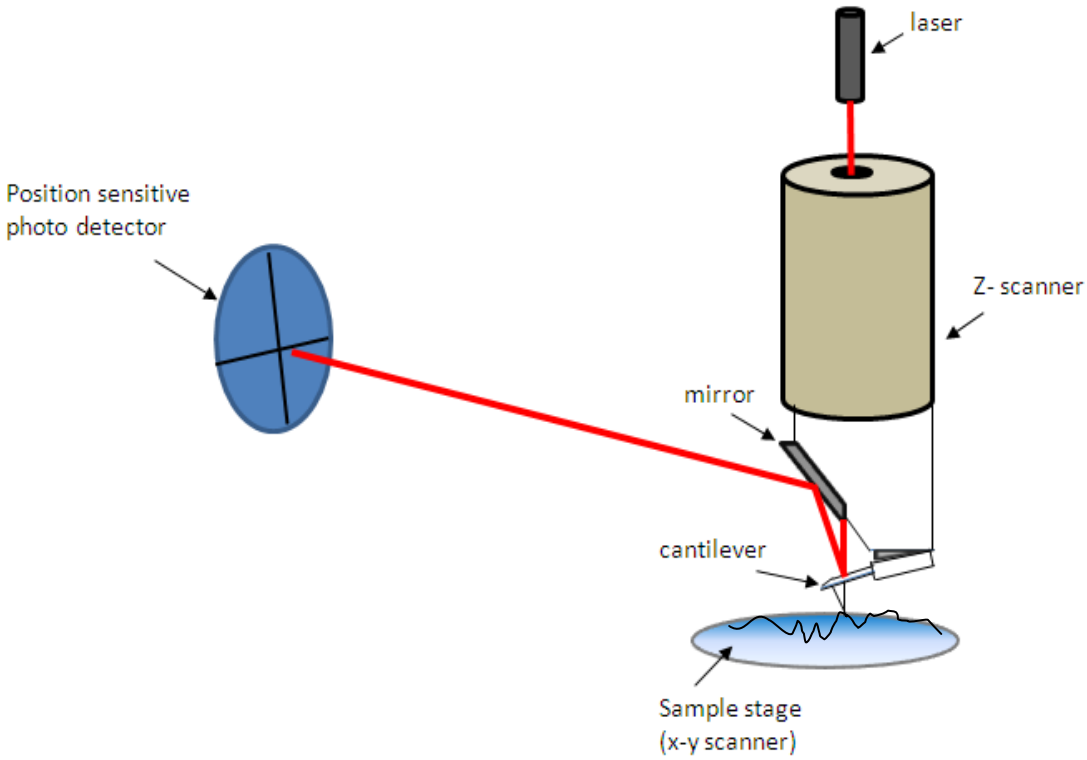

Figure 2.3 Schematic of the components of the AFM. The cantilever oscillations are detected by the position sensitive photo detector from the reflected laser beam. The signal is then transferred to the electronic components which control the data acquisition process, analysis and display of the results (Santos & Castanho, 2004).

The force interactions between the sample surface and the scanning tip cause bending, or even twisting of the cantilever. As it oscillates, a laser beam is reflected off its back (usually coated with a thin gold film for better reflection) and onto a position sensitive photo detector (PSPD). The image is obtained from the changing position of the reflected laser beam on the PSPD as the surface of the sample is scanned.

While scanning the sample, the AFM maintains a constant force between the tip and the samples so that at any one time, the distance between the two is always same. Since this force can be regulated, it is possible to take images at high or very low force values.

The scanning itself can be done in either one of two ways; by moving the sample stage in instances where the AFM has a piezoelectric scanner stage while the tip remains in a fixed position or by having the stage in a fixed y-axis position while the tip is either approached or retracted. In both cases, the distance between the tip and the sample is regulated by recording the force interactions.

2.2.3 Working modes of the AFM

The AFM can be operated in one of three ways depending on the force interactions between the tip and sample. In contact mode, the tip is brought into contact with the surface and the cantilever deflection is kept constant by the feedback loop. As the tip is in contact with the surface, it is possible that the sample may be damaged especially if it is soft, like in biological samples. For this, usually softer cantilevers with higher force constants are used.

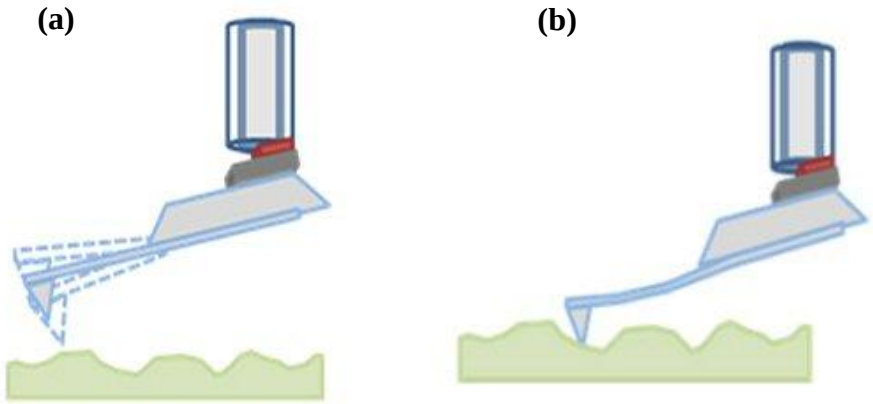

Figure 2.4 Illustration of (a) non-contact and tapping mode and (b) contact mode of the AFM

In non-contact mode, the oscillating tip is brought close to, but not touching, the surface of the sample. In this position, it is the van der Waals forces between the tip and sample that affect the oscillating frequency of the cantilever. By maintaining a constant

oscillation frequency and amplitude through the feedback loop, an image is obtained as the surface is scanned. For this mode, the cantilevers used are usually stiff.

Finally, there is the dynamic, or tapping mode, where the tip is operated the same as in the non-contact mode but at the same time is periodically brought in contact with the surface of the sample. In this mode, the oscillation amplitude of the cantilever is much greater than that in the non-contact mode, but the frequency of oscillation is damped by the repulsive forces that are dominant when the tip gets in contact with the surface.

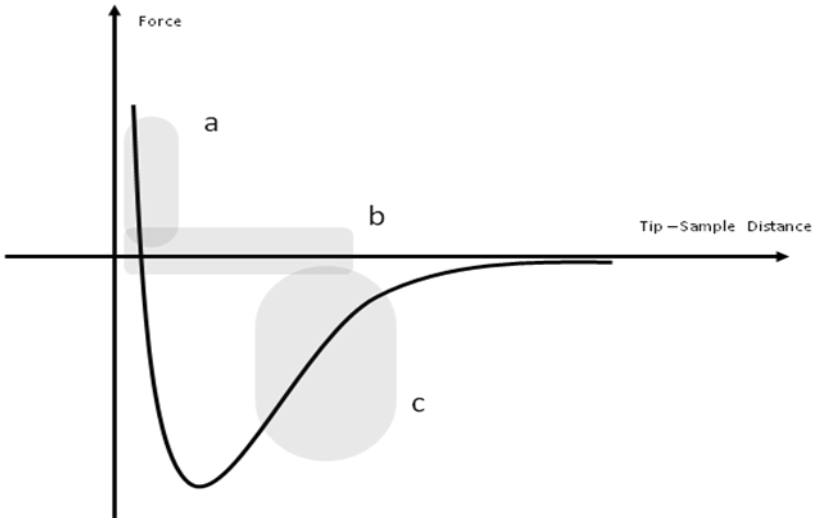

Figure 2.5 Plot of Force Versus Tip-Sample Distance showing regions where the different modes of the AFM would be applied. In (a) repulsive forces are dominant, so it is the contact mode region. In (c) attractive forces dominate, so non-contact mode is used. In (b) tapping mode is applied.

The AFM can also be used to image in liquids. This is significant as it makes possible the imaging of biological samples in near natural conditions. However, the liquid medium introduces other forces into the equation.

The viscoelastic forces cause extra damping to the oscillating cantilever and there are also additional capillary forces between the tip and sample. For these reasons imaging in solution is best done with the Contact mode.

2.2.4 Biological Samples and Substrates

Although imaging with the AFM is relatively simple, the final results depend a lot on the initial sample preparations. This includes having the correct substrate for immobilization of the sample and the right sample concentrations and conditions (whether in air or in solution). For the substrate, the main conditions are that it should be atomically flat, rigid and the subject to be studied should have a high adhesion to it. In the studies of biological samples with the AFM, two materials are usually used as the substrate, highly oriented pyrolitical graphite (HOPG) and mica. Both of these require no preparation prior to the deposition of the sample. Simply cleaving them yields atomically flat surfaces of considerable area virtually devoid of defects (Morris, 2010). In our study, we used mica which happens to be polar, negatively charged and to have a high adhesion to biological samples (Collagen proteins).

The sample is then applied onto the substrate by, in our case, direct adsorption. This means that a droplet of several microlitres of the sample is deposited directly onto the substrate and let to adsorb for several minutes. After this, the unbound material is rinsed off with the same buffer solution that was used to dissolve the protein. After adsorption, the sample can either be imaged with the AFM under the buffer solution in physiological conditions or let to dry and imaged in air. For imaging in air, the sample should be rinsed with distilled water to wash off salts and other contaminants and then dried off with an air flow.

2.3 Single Molecule Force Spectroscopy (SMFS)

More than topographical imaging, the AFM can be used to study force interactions between the tip and the sample. These can then be applied to investigate the chemical and mechanical properties of the sample like adhesion, elasticity and even bonding forces between molecules. One such application involves force curves which typically show the vertical displacement of the cantilever relative to the force applied as it is brought close to and then drawn away from the sample of the surface (Figure 2.7).

At the molecular level in most biological structures, it is now known that most of the macromolecules have load bearing functions e.g. collagens in cartilage. Therefore, application of controlled forces on single molecules serves to provide vital information

on their structure, dynamics and functions. This knowledge on the mechanics at the single molecule level of course leads to better understanding of the macrostructures.

For single protein molecules, force spectroscopy is best demonstrated by the "tack and pull" approach. In this method, the proteins are allowed to adsorb onto the mica substrate and after adsorption, placed into the liquid cell under the AFM. The AFM tip is then pressed down onto the surface and a force curve is obtained as the tip retracts. In this manner, a molecule might get attached to the tip and get stretched as the tip is retracted.

SMFS is based on simple force-distance spectroscopy as demonstrated in Figure 2.6, a simplified force-separation curve. Using this approach, the elastic properties of a material can be examined. By applying it to single polymer molecules, as illustrated in Figure 2.7, we can examine the single molecule mechanical characteristics and other additional properties.

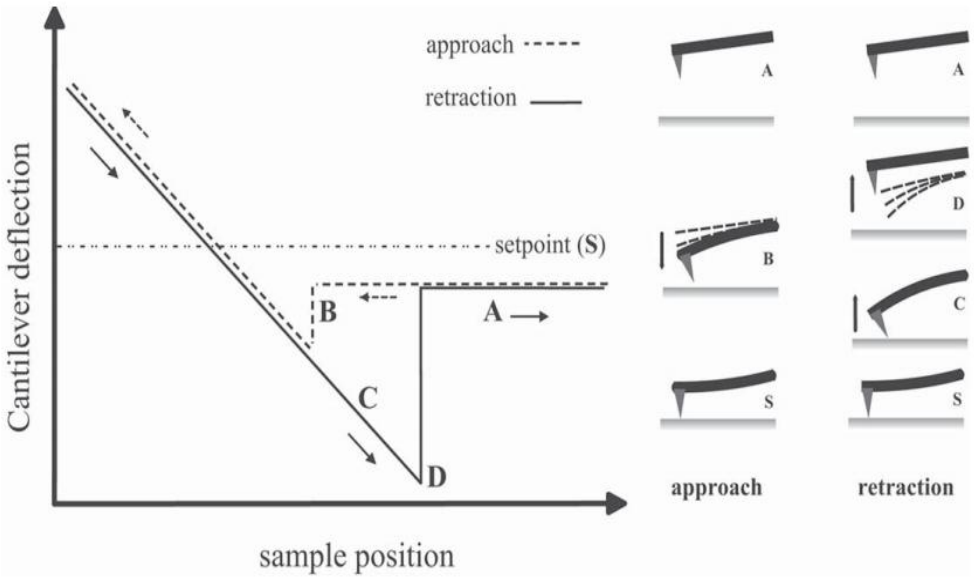

Figure 2.6 Idealized force curve and cantilever behavior: From A to B, the tip is approaching the surface. At B contact is made ("snap in"). After B, the cantilever bends until it reaches the specified force limit that is to be applied (S). The tip is then withdrawn towards C and D. At D, under the retraction force, the tip detaches from the sample ("snap off"). Between D and A, the cantilever returns to its resting position (Ricci, 2004).

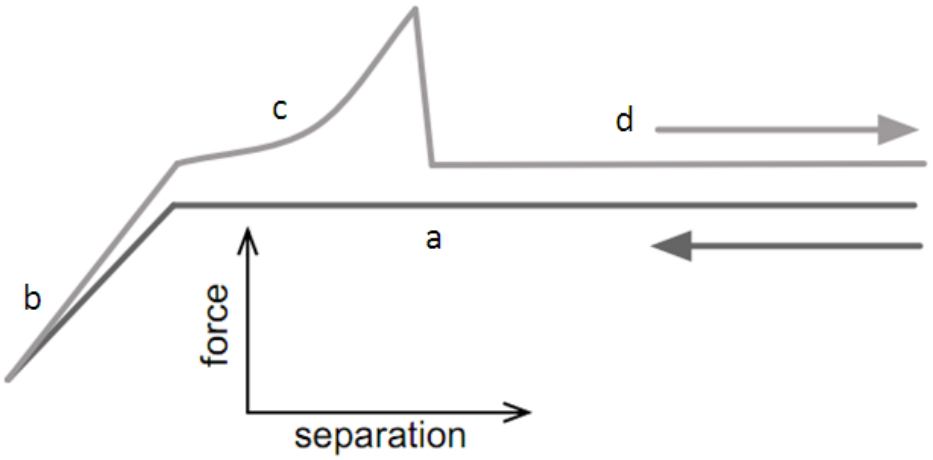

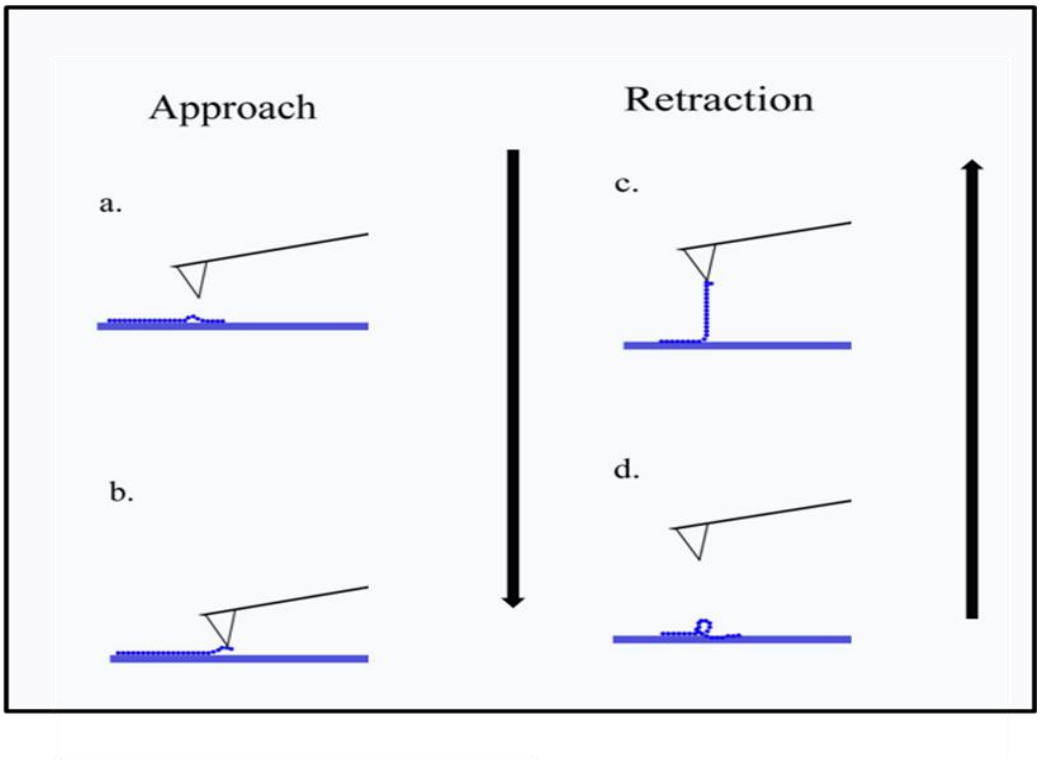

Figure 2.7 Illustration of idealized SMFS force curve. (a)The tip approaches the sample with zero deflection. (b)It makes contact at a predetermined set point and then starts to retract. (c)If there is a bond made, the cantilever will be deflected as it retracts. (d)When the restoring force of the cantilever exceeds the bonding force, rupture occurs and the cantilever continues to retract.

To optimize the results from SMFS experiments, either high constant forces (10-40 nN), or long contact duration times (1-3s) have been advocated. Others have simply

applied the normal force-distance cycle and seen it to be sufficient in picking up molecules (Morris, 2010). For reliable results, the experiment should ideally be carried out multiple times to provide adequate data for statistical analysis. From the force distance curves, the properties of the stretched protein can then be worked out by fitting to theoretical models.

2.4 Polymer Analysis Models

Single molecule proteins can be characterized as polymeric i.e. a string of monomers free to move around the inter-monomer linkages. As the monomers add up to increase the size of the polymer, their flexibility around the links also decreases. Such polymers are termed semi-flexible coils. There are two theoretical models to describe the stretching of these semi-flexible polymers: the Kratky-Porod Worm Like Chain model (WLC) and the Freely jointed Chain model (FJC) (Graham, 2004; Janshoff, 2000).

2.4.1 Freely Jointed Chain Model

This model assumes that the polymer is subdivided into a number **N** of rigid segements of length ***l*** (termed the Kuhn Length).these are connected to each other through flexible joints. The contour length of the molecule in this model is determined from the Langevin Function, ***L***, and is defined as **L=N*l*** (the contour length being the full unextended length of the polymer) (Janshoff, 2000).

For small extensions, the extension due to force applied in this case is formulated in its practical form as:

$$\mathbf{x(F) = L\left[\coth\left(\frac{Fl}{k_B T}\right) - \frac{k_B T}{Fl}\right]} \qquad (3.1)$$

Here ***F*** is the force applied, ***l*** the Kuhn length, k_B the Boltzmann Constant, ***L*** the contour length and ***T*** absolute temperature.

For larger extensions, additional bonds and bond deformations within polymers have to be included and so the FJC is expanded to:

$$x(F) = L\left[\coth\left(\frac{Fl}{k_B T}\right) - \frac{k_B T}{Fl}\right]\left(1 + \frac{F}{E}\right) \tag{3.2}$$

Where $\boldsymbol{E}$ is stretch modulus of the segment defined from Young's Modulus as $\boldsymbol{E} = \boldsymbol{AY}$, with $\boldsymbol{A}$ the cross-sectional area of the segment (Graham, 2005).

2.4.2 Worm Like Chain Model

Whereas the FJC assumes that the polymer is a chain of rigid rods connected by freely rotating joints, the WLC approaches from a point assuming uniform flexibility over the whole length of the polymer. The WLC model provides the best approximation for the description of biopolymers and their stretching behavior.

The WLC is formulated as:

$$F(z) = \frac{k_B T}{l_p}\left[\frac{1}{4}\left(1 - \frac{Z}{L_c}\right)^{-2} + \frac{Z}{L_c} - \frac{1}{4}\right] \tag{3.3}$$

Where $\boldsymbol{F}$ is the force applied, $\boldsymbol{l_p}$ is the persistence length (distance between the start and end points), $\boldsymbol{L_c}$ is the contour length (total end to end distance for a fully elongated chain), $\boldsymbol{z}$ is the extension, $\boldsymbol{k_B}$ the Boltzmann constant and $\boldsymbol{T}$ absolute temperature. This is the most common version of the WLC that appears in literature although it has some modifications to deal with shortcomings in specific situations (Graham, 2005; Morris, 2010).

By fitting the experimental force-extension data to the WLC model, the characteristic polymer chain properties of contour length $\boldsymbol{L_c}$ and persistence length $\boldsymbol{l_p}$ can be determined.

CHAPTER 3

EXPERIMENTAL AND ANALYTICAL METHODS

All chemicals (reagent grade) were purchased from Sigma Aldrich and used as received.

3.1 Extraction of Collagen Type II

Type II collagen was extracted from bovine cartilage which was obtained from a local abattoir. There are several protocol available in literature (Kuo, 2005; Brodsky, 1982) about the extraction of collagen type II. Generally pepsin or diluted acids are used to digest the proteins from the tissue (Pieper, 1998). In this work, the extraction was carried out with pepsin and the details of the protocol are as follow:

1. Using a scalpel, cartilage tissue was sliced from the bovine femur bone and washed with deionized water to remove any blood residue.
2. The cartilage was cut into small pieces and then using a blender, was minced into even finer pieces. This was done in cold distilled water with some ice chips so as to maintain the cartilage temperature at levels below $4^{o}C$.
3. To separate the water, the cartilage was centrifuged at 5000g at $4^{o}C$ for 50-60 minutes using a centrifuge. After separation, the minced cartilage was stirred overnight at $4^{o}C$ in 10ml of Guanidine-HCl per gram of minced cartilage.
4. Next, the cartilage was collected by centrifuging in 15ml tubes for 30 minutes at 5000g at $4^{o}C$, then discarding the supernatant. This was done three times, each time adding 10ml of cold distilled water per gram of cartilage and centrifuging then discarding the supernatant. This step removes much of the proteoglycans.
5. The cartilage pellet was suspended again in 30 ml 500mM acetic acid with pH adjusted to 2.8.

6. To this suspension, pepsin was added in the ratio of (pepsin:cartilage) 1:20 (weight/wet weight) and stirred gently for 36 hours in the cold. The pepsin digests the cartilage to release soluble collagen Type II.
7. The solubilized collagen was separated from the cartilage residue by centrifuging at 5000g for 30min at 4^{o}C and discarding the pellet.
8. To the supernatant, 5M NaCl was added slowly, over a 30 minute period, to a final concentration of 0.8M. The collagen was then allowed to precipitate for 24 hours at 4^{o}C.
9. To recover the precipitate, the solution was centrifuged in 15ml tubes for 60minutes at 5000g at 4^{o}C. This precipitate was then dissolved in 20ml of 0.1 M acetic acid by stirring overnight at 4^{o}C.
10. To remove any insoluble material, the solution was centrifuged for 1 hour at 5000g.
11. The solution was then dialyzed against several changes of 10 mM Na_2HPO_4 at 4^{o}C using MWCO 10000 dialysis tubing.
12. The final solution was then kept at 4^{o}C until it is used for further analysis.

To check for the presence of collagen Type II in the solution, gel electrophoresis and Raman Spectroscopy were used.

3.2 Determination of Collagen Type II Purity via SDS PAGE

Once the collagen was extracted from cartilage, a purity test is required to assure that the end product is actually clean collagen type II without other contaminants. The purity of isolated collagen can be analysed using sodium dodecyl sulphate poly-acrylamide gel electrophoresis (SDS-PAGE) (Pieper, 1999; Pieper, 2002). SDS-PAGE is a method used to separate proteins according to their size. Since different proteins with similar molecular weights may migrate differently due to their differences in secondary, tertiary or quaternary structure, an anionic detergent (SDS) is used in SDS-PAGE to reduce proteins to their primary (linear) structure and coat them with uniform negative charges.

Procedures for SDS-PAGE generally involve: (1) making a gel and assembling the gel apparatus, (2) mixing protein samples with sample buffer containing SDS and

heat the mixture at high temperature, (3) loading samples and running the electrophoresis, (4) fixing and staining the separated proteins (Shapiro, 1967).

The SDS PAGE protocol used in this work is briefly as follows: Collagen was partially dissolved by denaturation at 95°C for 5 min under reducing conditions (5% (w/v) 2-mercaptoethanol). The denatured collagen was loaded on an 8% (w/v) gel and visualized by staining with a Coomassie Brilliant Blue solution (0.1% (w/v)). SDS PAGE indicated that the isolated collagen was essentially free of other proteins. The molecular weight of collagen type II was found to be around 140 kDa, which is in good agreement with the literature values (Pieper, 1999).

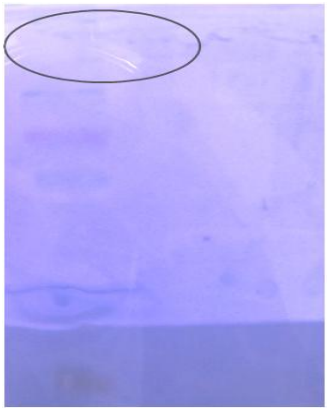

Figure 3.1 Image of SDS gel showing molecular weight bands with the collagen Type II having a (faded) band at approximately 140 kDa (circled area).

3.2 Raman Spectroscopy of Collagen Type II

Raman spectrum of collagen type II was recorded on a Thermo-Scientific DXR Raman microscope (Thermo, Madison, WI). The 780 nm laser beam (maximum output of 150 mW) was focused onto sample with a beam size of 0.8 μm via an Olympus 100X with 0.95 NA (numerical aperture) microscope objective. The Raman spectrum was acquired by a TE cooled (at −50°C) CCD detector. The spectral resolution of the Raman microscopy is 2 cm^{-1}. The Raman spectrum was collected with an integration time of 20 s and a 785-nm laser illumination power of 20 mW on the sample.

A 20μl aliquot of Collagen solution was sprayed onto a quartz microscope slide in order to acquire a Raman spectrum of Collagen type II. Figure 3.1 shows the Raman spectrum of Collagen Type II with 780 nm laser illumination. Raman peaks were

observed at the following locations: 854.24, 875, 938.48, 1060.60, 1164, 1244.42, 1382.37, 1446.09, 1553.82, 1597.77and 1666.77 cm^{-1}. Table 1 outlines the tentative biochemical assignments of respective Raman peaks of Collagen type II (Natalie, 2011; Kareshi, 2010).

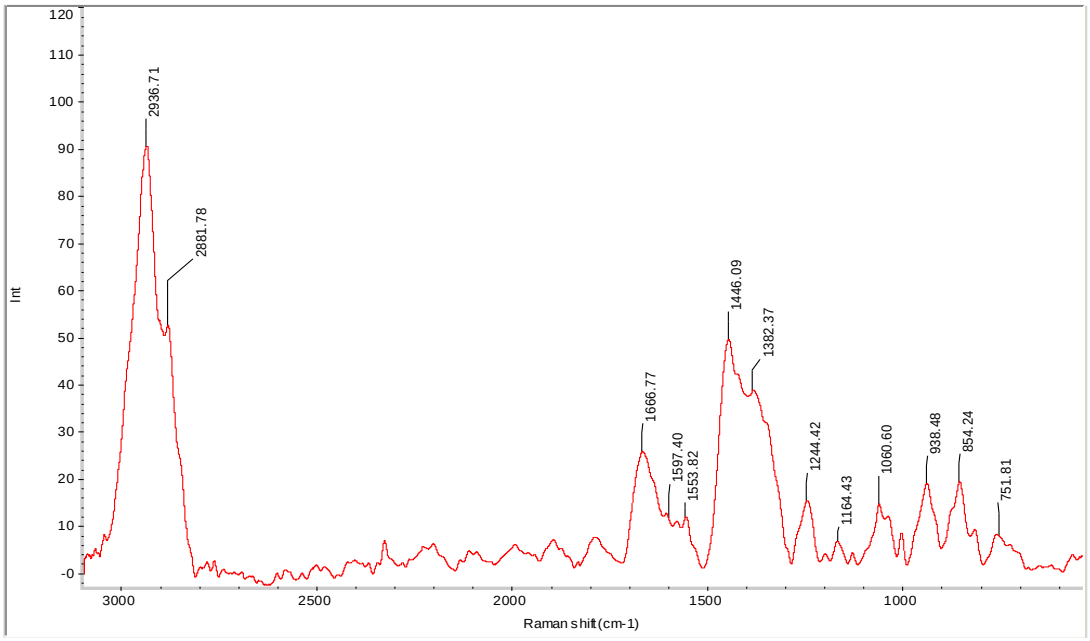

Figure 3.2 The Raman spectrum of Collagen Type II with 780 nm laser illumination

Table 3.1 The assignments of observed Raman peaks of Collagen Type II

Peak Position (cm^{-1})	Assignments
854	(C-C) stretch, proline ring
875	(C-C) stretch, hydroxyproline ring
938	(C-C) deformation, aggrecan/(C-O-C) stretch, GAG
1003	(C-C) symmetric ring stretch; phenylalanine
1060	Pyranose ring
1164	Pyranose ring
1244	(C—N) stretch alpha-helix; amide III
1446	(C-H) bend; protein CH_2, CH_3 scissor
1553	amide II
1597	(C=O) stretch alpha-helix;
1666	Amide I

3.3 AFM measurements

The AFM measurements were acquired using a Park AFM (XE-100, Park AFM, Korea), supported on a Minus-K (25BM-6, Minus-K, Inglewood, CA) vibration isolation base. The Z detector sensitivity were calibrated according to the owner's manual (Park, 2008). Figure 4.9 shows the sensitivity calibration of the detector. The AFM the tips used in this work were calibrated following thermal calibration procedure (Park, 2010).

The AFM images were acquired with a commercial non contact Si tip with the nominal radius <10 nm, resonant frequency nominal of 330 kHz, a nominal spring constant of 42N/m (PPP-NCHR, Nanosensors, Switzerland). Images were acquired at a resolution of 512×512 points within the range of 0.5-0.8 Hz scan rate and were subjected to first-order flattening.

The AFM images in liquid were acquired with a commercial contact Si tip with nominal radius <10 nm, resonant frequency nominal of 21 kHz and nominal spring constant of 0.011N/m (HYDRA-2R NG, AppNano, USA).

3.4. SEM measurements

SEM images of cartilage were acquired with a JEOL NanoScope SEM. The cartilage sections were embedded in paraffin and sectioned using a Leica microtome. The sections were then set onto glass slides and were coated with a thin layer of gold film before the SEM imaging.

CHAPTER 4

RESULTS AND DISCUSSION

4.1 Cartilage Topography and Mechanical Properties

Bovine cartilage was sectioned using a scalpel from the femur of a freshly acquired knee joint. This was then set in paraffin and microtomed to get thin sections of approximately 1-3 μm. The thin sections so acquired were then placed on glass slides and imaged under both the AFM, and after coating with a thin gold film, under the SEM.

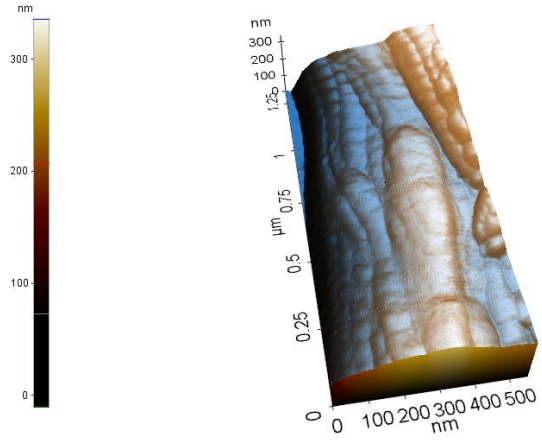

Figure 4.1 Non Contact Mode Scanned Image of Bovine Cartilage surface showing the underlying collagen fibril bands.

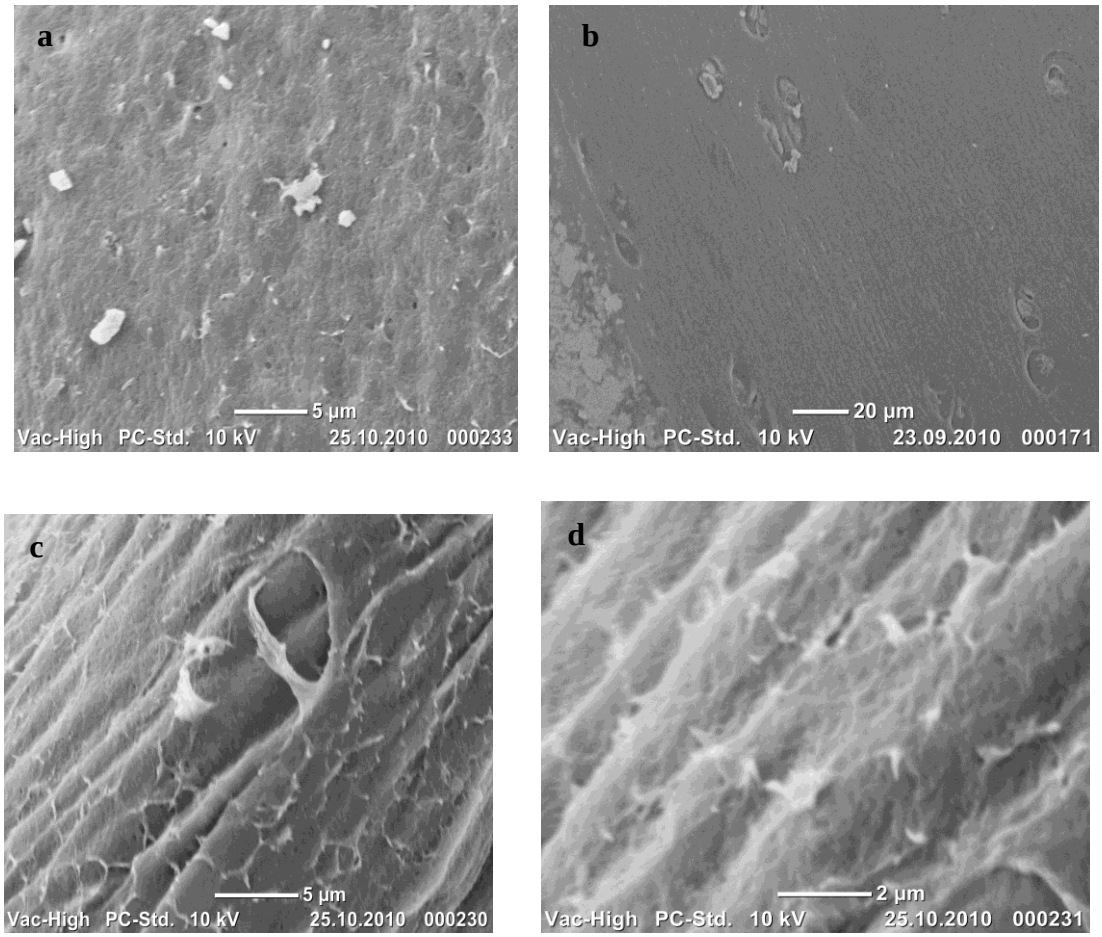

Figure 4.2 SEM images of gold coated lateral Cartilage Sections. In (a) and (b) a thinner gold film was applied. In (c) and (d) the thickness of the gold film was increased. Collagen network is more apparent in images (c) and (d)

For the sections of imaged under the SEM, it was possible to discern the fibril network of collagens, with the network becoming clearer at higher resolutions (see Figure 4.2. (c) and (d)).

The sections imaged under the AFM (e.g. Figure 4.3) were such that it was possible to see the single collagens that formed the fibril networks and even measure their dimensions.

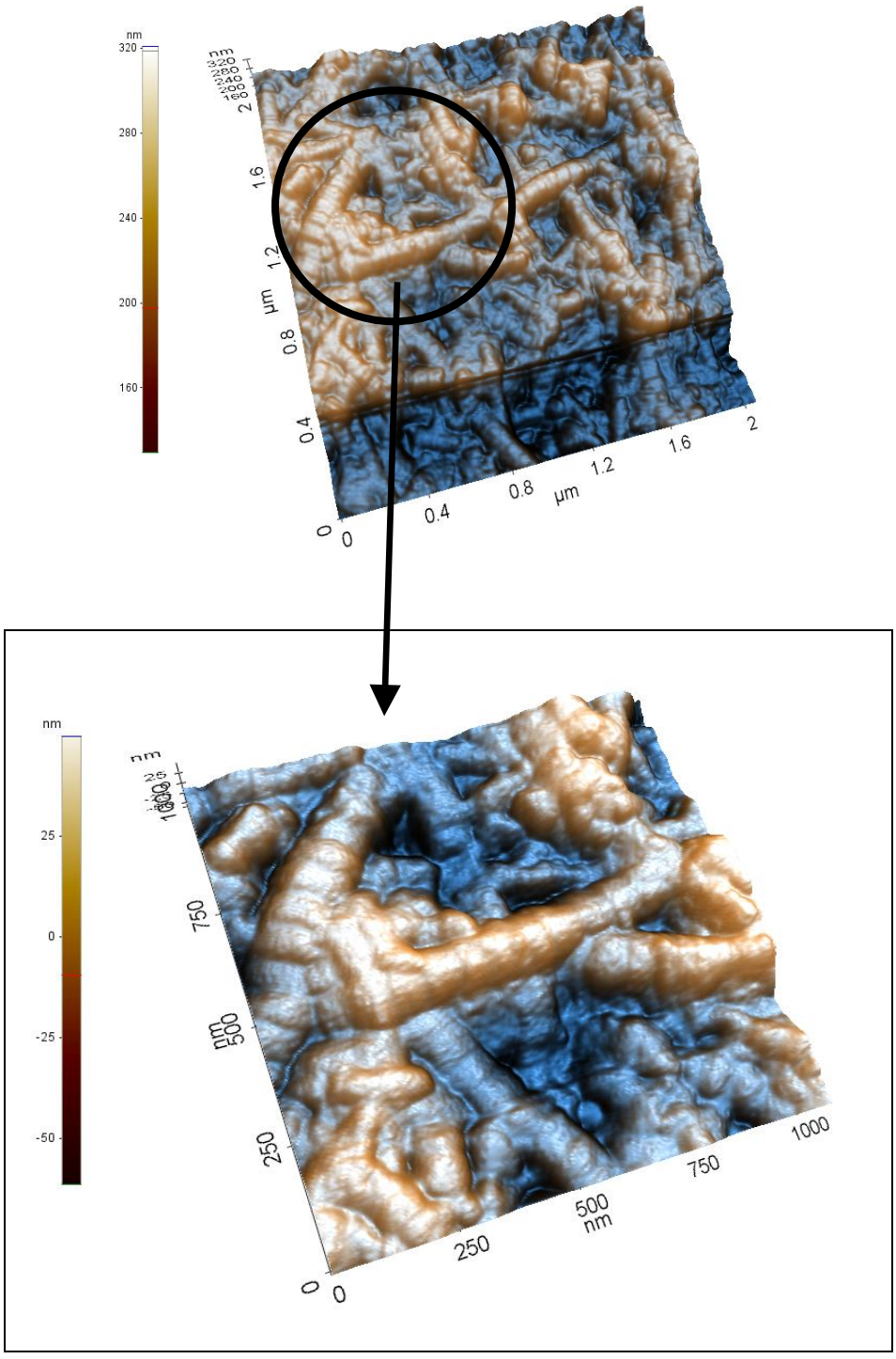

Figure 4.3 Non Contact Mode Scanned Image of Bovine Cartilage Sections showing the collagen fibril networks.

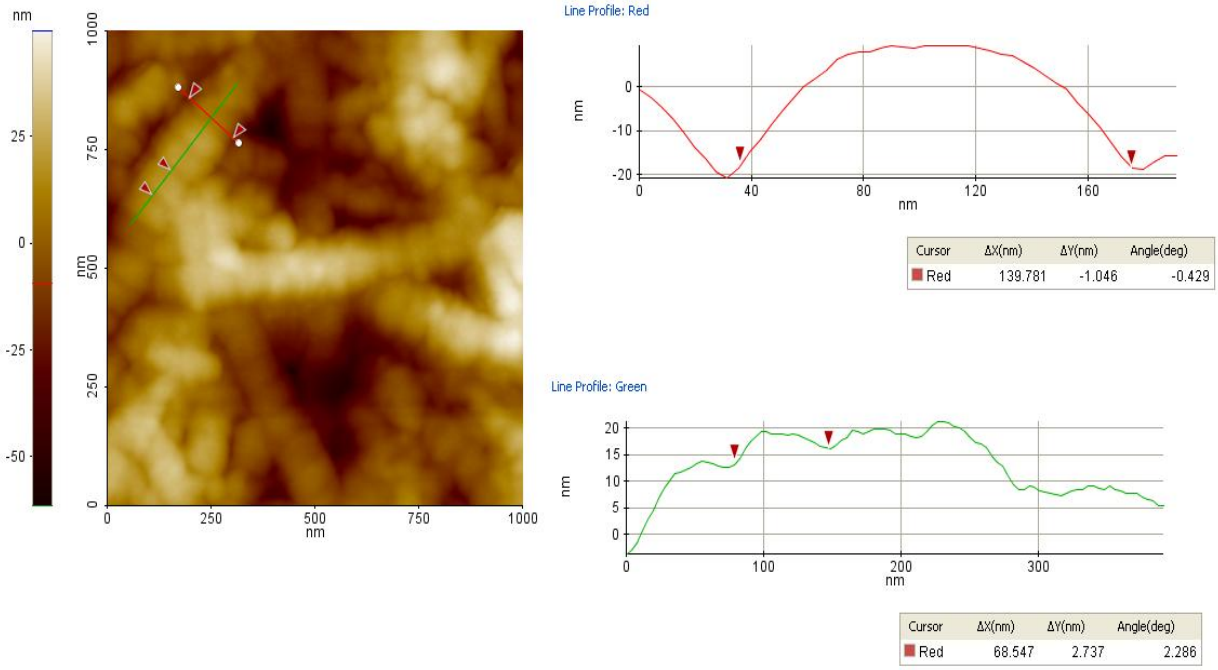

Figure 4.4 Non Contact Mode Scanned Image of Bovine Cartilage Sections showing the profiles of single collagen fibrils. The D-Banding was measured at 68nm and fibril width at 139.78nm.

By measuring the line profiles of the collgen networks that are visible from the AFM images of the cartilage sections (Figure 4.4), the D-banding was shown to be occuring at around 68 nm (compared to literature values of an average of 67 nm), and the diameter of a single collagen fibril came to around 140 nm.

After imaging with the AFM, a reference image from a section of the cartilage was taken in non-Contact mode from which Force Distance (FD) spectroscopy measurements were done. The force curves were acquired from a grid map (32 by 32 points, $5\mu m^2$) and the results as can be seen from Figure 4.5 gave a force-volume map together with images representing the adhesion energies, snap in energy and hardness in addition to topography of the cartilage surface.

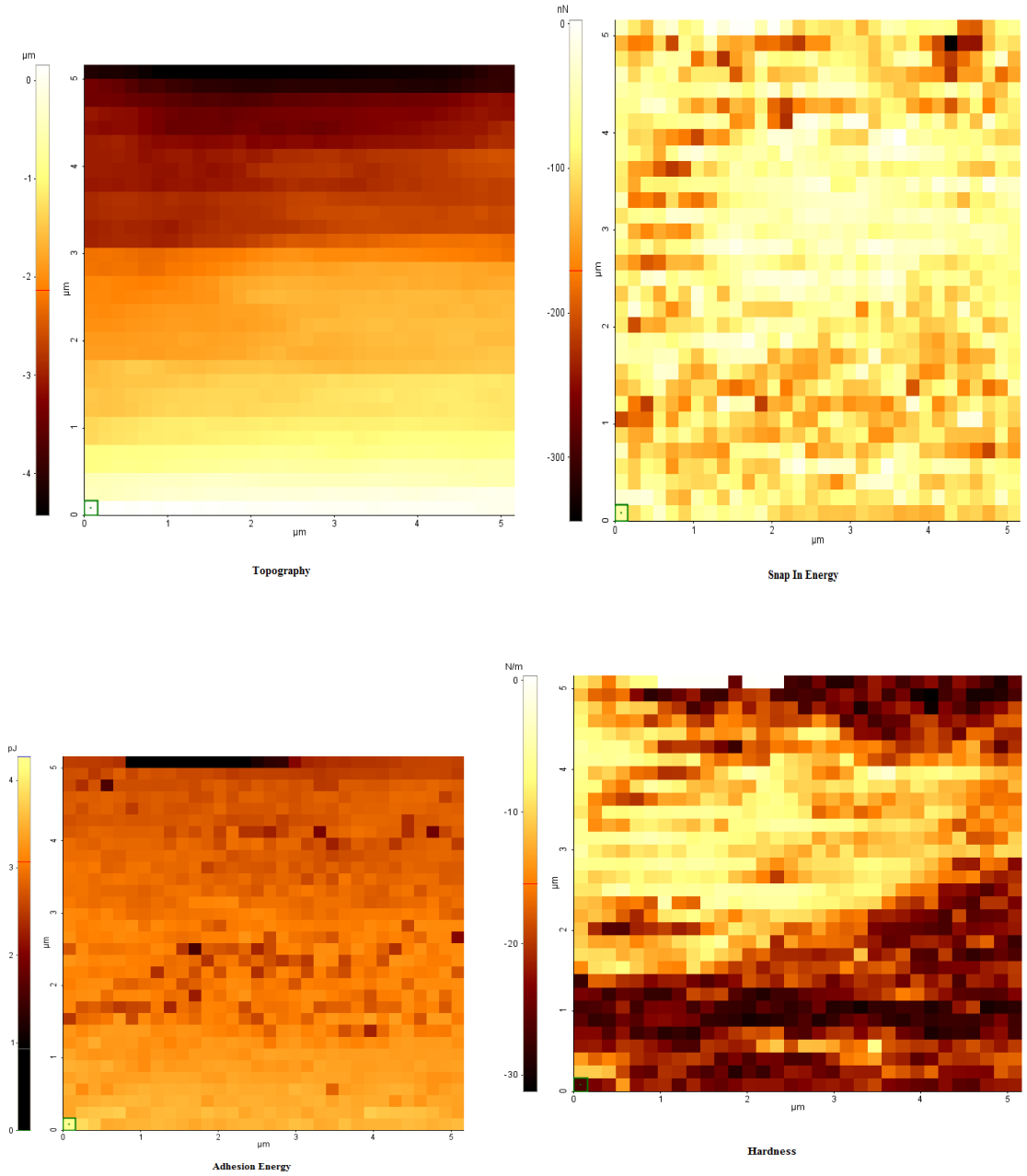

Figure 4.5 Force-Volume images showing in clockwise direction the Topography, "Snap In" Energy, Hardness, and Adhesive Energy of the mapped section. The images give a relative value for each point on the grid, with the whiter parts showing higher values for elevation, energy or hardness, while the darker regions represent lower values. That way it is possible to say, as an example, which points on the surface are harder, or have greater adhesive forces with the tip relative to the others.

4.2 AFM Collagen Type II Imaging

The collagens were imaged both in air and in buffer solution. In both cases, the contact mode was used. For imaging in solution, the cantilever had to be given some time before being used since the additional forces due to the liquid caused extra oscillations that affected measurements.

4.2.1 Effect of pH on Collagen Fibrillogenesis

From the initial solution of collagen in acetic acid, 40μm aliquots were taken and to these were added PBS buffer solution to a final volume of approximately 2ml. These solutions had their pH values adjusted so that we had solutions with pH 4, 6, 8, and 10 and were incubated at room temperature, approximately 24^{o}C. Collagens from each of these solutions were then imaged in air at different time periods (12 hours, 24 hours and 4 days) and the fibril formation behavior observed. Figures 4.6 illustrate the formation of the fibril network patterns at different pH with different incubation times, comparing the collagens at different pH after 12 hours and 4 days incubation.

The images obtained showed that for the first 12 hours at pH 4, the collagens aggregated to form granules on the mica surface. At pH 6, 8 and 10, the collagens reconstituted into fibrils, with the thickness and density of the fibrils formed increasing with increasing pH. After 24 hours incubation, the collagens at pH 4 were still aggregated although there was the occasional single fibril on the surface. At higher pH, the fibrils formed became more distinct, but still a bit dense, although at pH 6 they did not show the D-banding pattern characteristic of collagens.

In 4 days time, the collagens at pH 4 although still aggregated, had started forming into a fibril network. At pH 6, the network of fibrils was formed, with no aggregation but still the collagen fibrils showed no D-banding patterns. At pH 8, the fibrils had become longer and more isolated on the surface, forming no networks. The collagens at pH 10 had even longer fibrils, and they were spread even further apart on the mica surface. These results, which are summarized in Table 4.1, are consistent with what has been observed and recorded in literature (Friedrichs, 2007, Cisneros, 2006).

Table 4.1 Collagen Samples at different pH with different Incubation times

pH	12 hours Incubation	4 days Incubation
4	Granulation with scattered single fibrils	Beginnings of fibril network
6	Fibril network	Thicker fibril network
8	Fibril network	Single fibrils, no networks
10	Fibril network	Single fibrils but very isolated

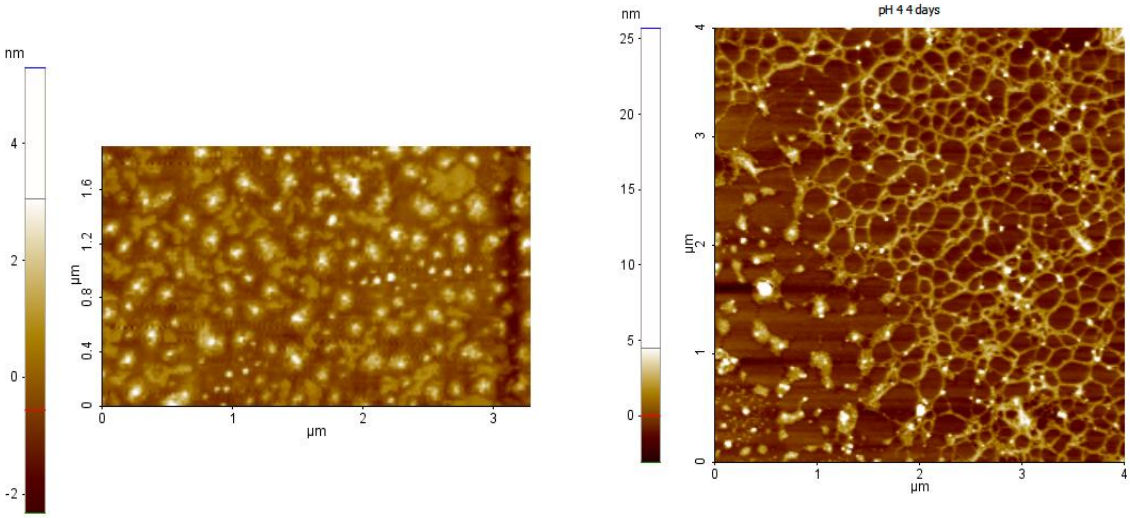

Figure 4.6 (a) AFM topography images showing from left to right collagen structure for incubation at pH 4 after 12 hours and 4 days respectively. After 12 hours, only granules are observed but there are the beginnings of a fibril network after 4 days incubation.

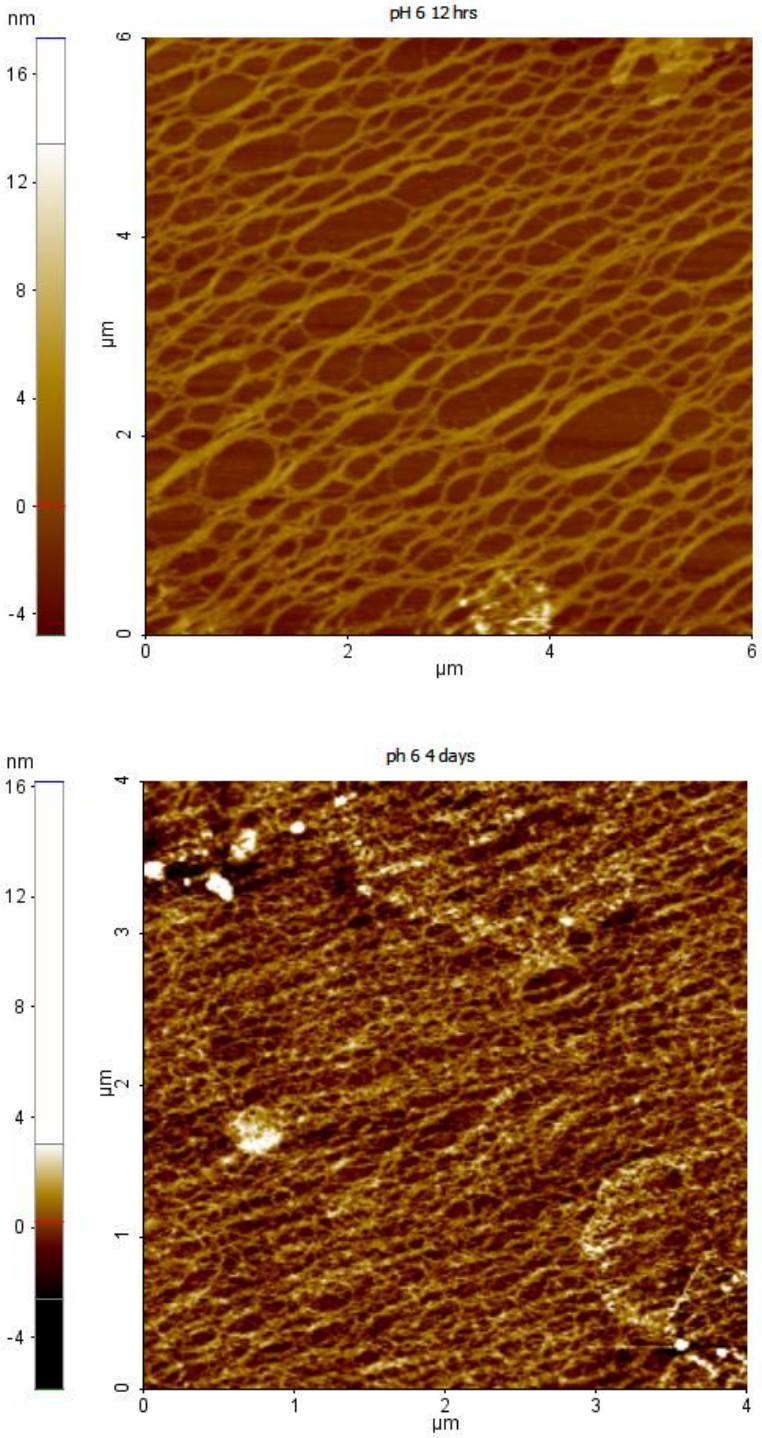

Figure 4.6 (b) AFM topography image fibril network formation after incubation at pH 6 for 12 hours with the network getting thicker after 4 days incubation.

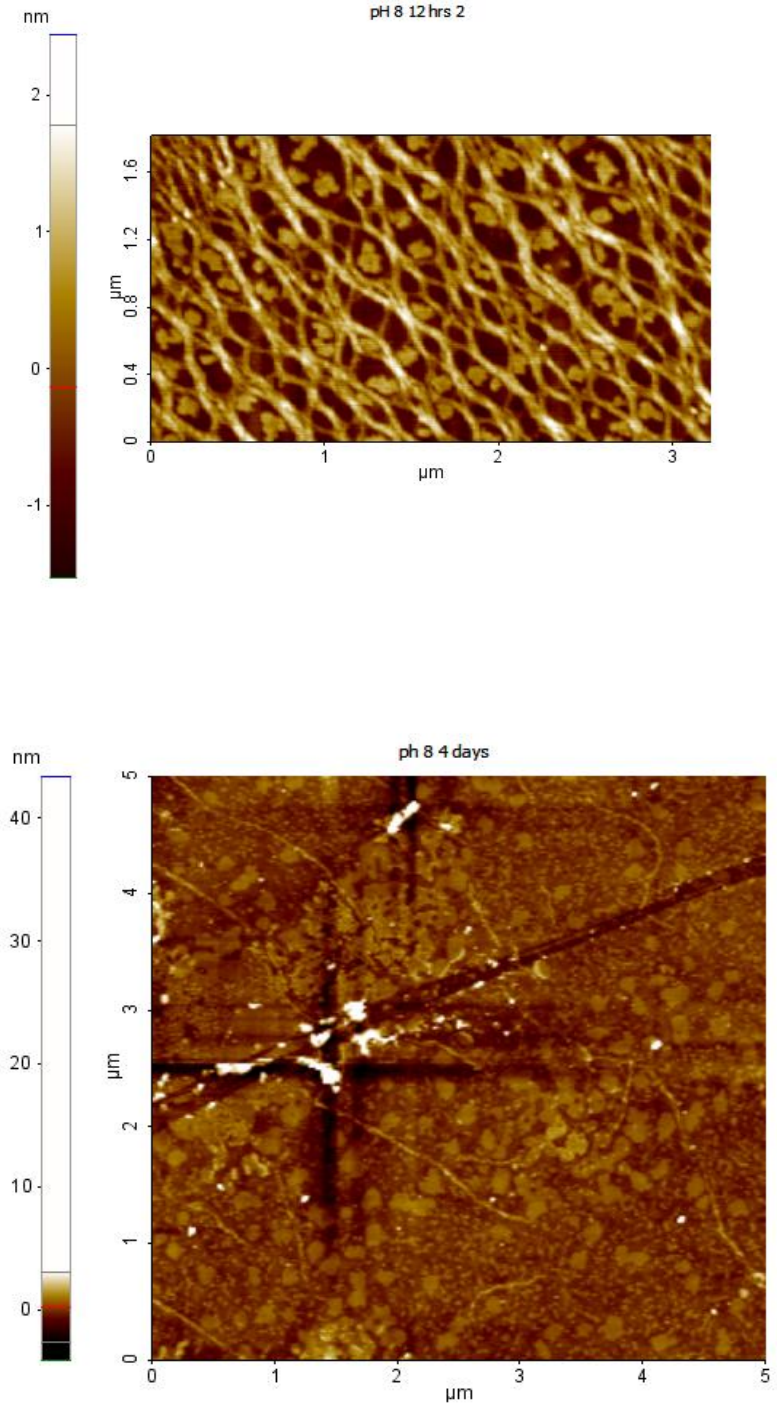

Figure 4.6 (c) AFM topography images showing isolated fibrils with no network formation after 4 day incubation at pH 8 as opposed to the fibril network that forms after incubation for 12 hours.

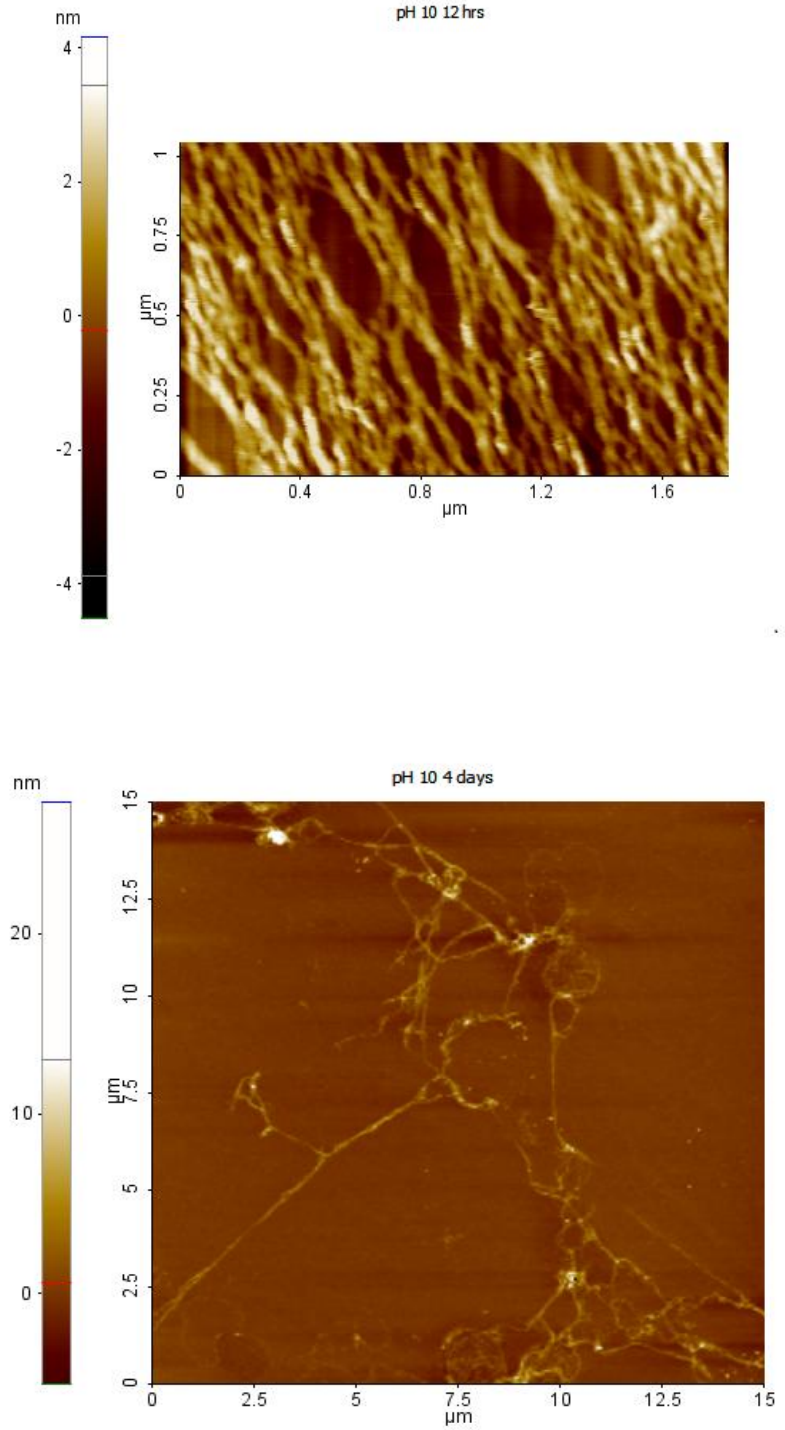

Figure 4.6 (d) AFM topography images showing greatly isolated fibrils with no network formation after 4 day incubation at pH 10. The fibril network is seen only after incubation for 12 hours.

4.3 SMFS and WLC Fitting

After imaging the collagens at different pH and analysing their different topographical properties as they presented, the next step was working out their mechanical properties. This was done by recording the force-extension curves for single molecules stretched by the AFM tip.

To ensure the mica substrate was totally covered with the proteins, around 30ml of Collagen Type II dissolved in PBS containig 0.1 M acetic acid at a concentration of 0.1mg/ml was deposited on the surface. The solution was at pH 8. This was let to rest for a few minutes before rinsing with PBS buffer and then being placed into the liquid cell. The experiment was carried out under PBS buffer solution. Figure 4.7 shows the initial refence image taken in contact mode. The force-extension experiments were carried out on different points with measurement taken from each point at least 10 times to a cumulative number of at least 100 force-extension curves.

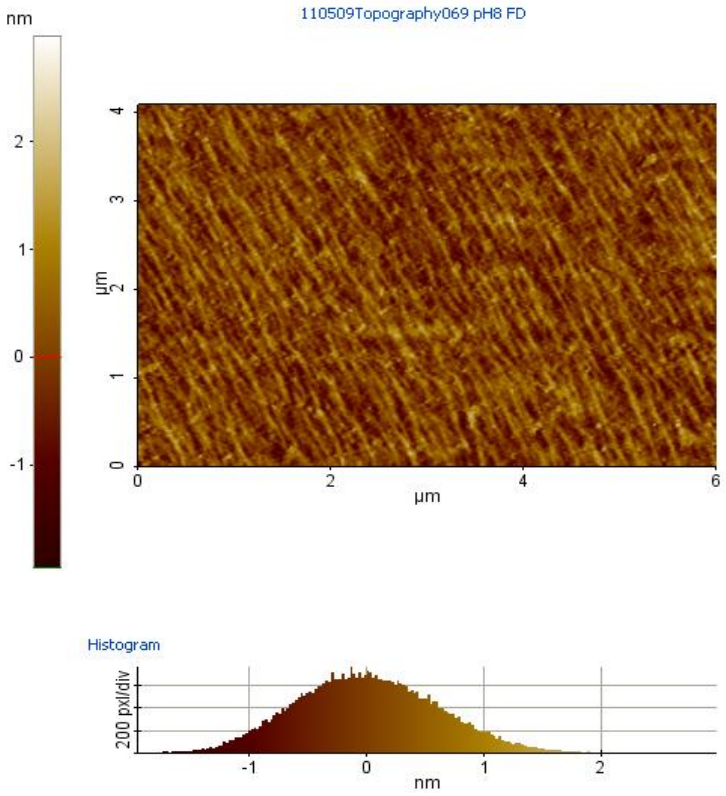

Figure 4.7(a) AFM topography image showing fibril network for the reference image for SMFS measurements. The histogram shows a fibril thickness of approximately 2nm.

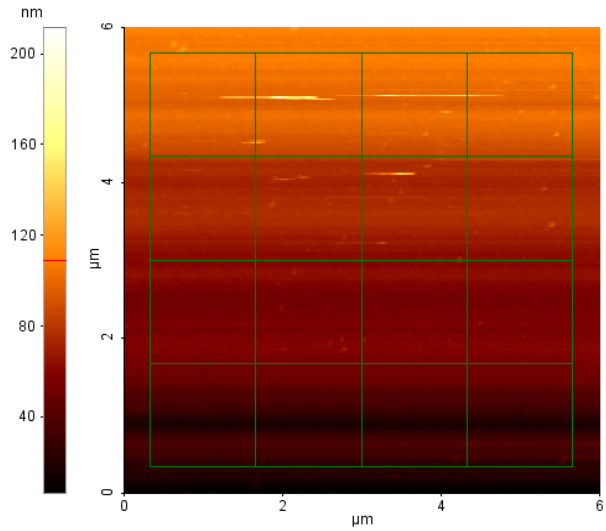

Figure 4.7(b) AFM topography image showing reference image grid points for SMFS measurements.

The force-separation curves obtained from the measurements were similar to patterns observed by others who carried out similar experiments on the stretching of macromolecular collagen complexes (Graham, 2005, Bozec, 2005). In Figure 4.8, the initial force-separation curves obtained are shown. The stretching analyses are done on the retrace (red) curve, after changing the forces from (a) so they take the form of (b).

(a) (b)

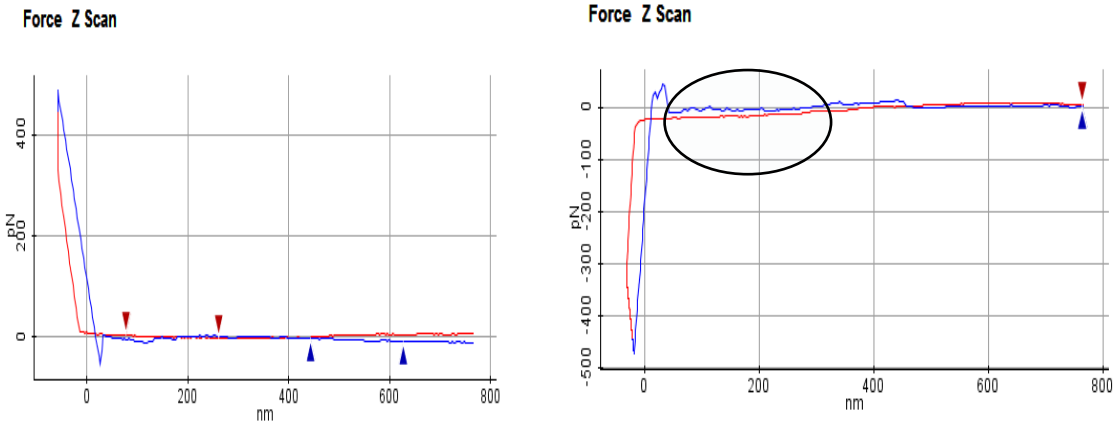

Figure 4.8 Force – separation curves of collagen type II obtained from the pulling experiments. In (a) the forces are actually negative so that the curve takes the form (b) when the forces are set positive. The highlighted area in (b) shows the region where fitting to theoretical models was done.

As with the others, the force curves we observed had stretching peaks that occurred after the tip had been retracted some distance rather than as soon as the tip left the surface. This phase can be assumed to be the point where the monomer is straightening, and the force is only detected once it is fully extended and begins to be stretched.

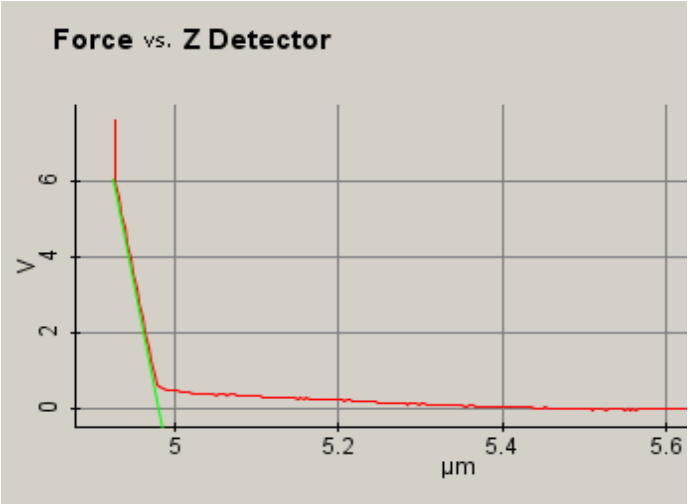

Figure 4.9 Determination of the sensitivity of the Z-detector. The red line is a representative F-D curve. Green line shows the fitted data. Sensitivity was calculated as 108.28 V/µm

After obtaining the curves, we were able to determine firstly the sensitivity of the Z detector i.e the amount of force that could be measured as it retracted for every unit of separation as illustrated in Figure 4.9.

Since the tip underwent no functionalization before the experiment to specify the collagen-tip coupling, there was no guarantee that a just single molecule was being pulled at any one time. The mechanics of the collagens can only be understood fully, however, only if it is clear whether multiple or single proteins are being pulled. The curve itself can either come out in one of two ways: as a single unique stretching peak which is proof of single molecule stretching or as a complex series of stretching peaks (Bozec 2005).

Of the curves obtained from repeated Force-distance measurements, we considered the ones showing clear stretching peaks as being the responses of single monomers being stretched. The data was fitted to the WLC to give us a contour length of 209 ± 41 nm.

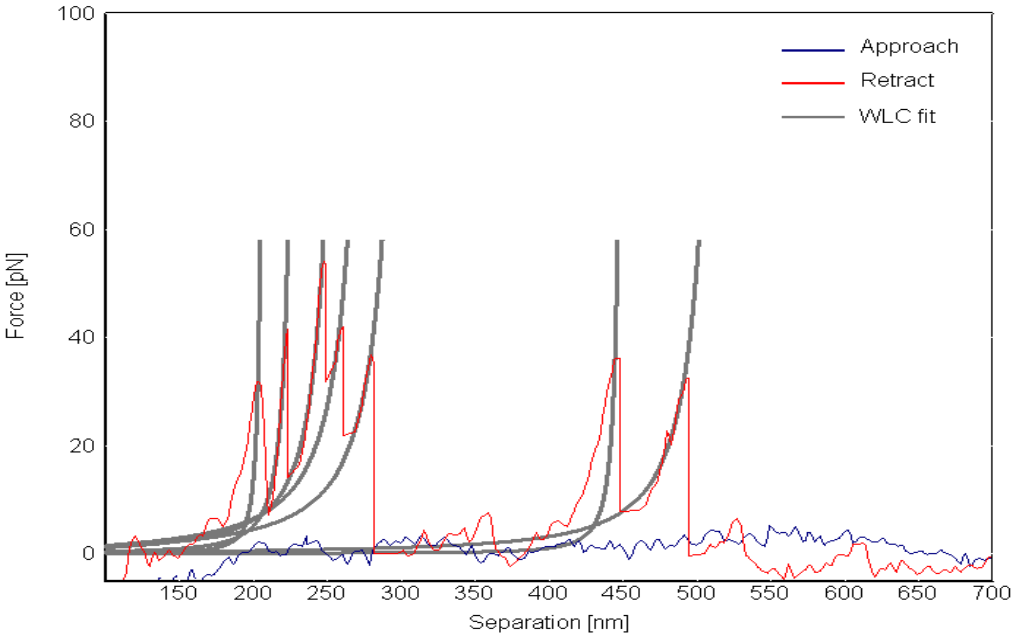

Figure 4.10 Force – separation curves of collagen type II showing the fitted regions. The data were fitted to the WLC model and Contour length was found to be 209 ± 41 nm with persistence length of 11.72 nm.

The information that can be gathered from the fitted curves (seen in Figure 4.10) is that contrary to what has been previously assumed, the Type II collagen is not actually a rigid rod. The ratio of the persistence length to the contour length observed from our experiments can be interpreted to mean the molecule is quite flexible. The multiple peaks as seen from the curve also imply either the pulling of more than a single molecule for each point or the unfolding of the D-banding structure of the molecules (the peaks appear at intervals of between 50-100 nm and this is characteristic of the D-banding pattern which happens at average intervals of 67nm).

CHAPTER 5

CONCLUSION

Articular cartilage is principally made up of a collagen fibril network that acts to attenuate the tensional forces within the structure when the proteoglycan gel, also part of the cartilage, swells to increase the pressure. As such, any observed mechanical properties of the cartilage really depend on the dimensional level at which the investigations are made. More detailed information on cartilage mechanics and structural make up can be provided from measurements at the nanometer scale. From this we can get that those physical or chemical changes that would cause the onset of cartilage diseases like OA can be detected early from investigation of the nano-mechanical and structural properties of the collagens (specifically collagen type II).

In order to get more information on their structure and nano-mechanical properties i.e. elastic modulus, collagen type II molecules were investigated with the AFM. Additionally, the effect of buffer solution pH together with incubation periods at room temperature, 23^{o}C, on the collagen type II fibril formation was investigated. For the pH studies, the collagen was dissolved in PBS buffer solution containing 0.1 M acetic acid with the pH adjusted using 0.1 M NaOH to 4, 6, 8 and 10. The different samples were incubated at room temperature and imaged after 12 hours, 24 hours and 4 days. The AFM images were taken in ambient conditions and the results showed consistency with earlier observed results in literature (Gelse, 2004).

For the spectroscopy measurements of the collagen type II, the collagens were investigated under buffer solution. The resulting curves were fitted using the WLC to give a contour length of around 209 nm with a persistence length of 11.72 nm. Again, these results show consistency with what has earlier been observed in literature (Rich, 1955; Bozec, 2005).

More than just being an important part of the structural make up of cartilage, collagens in general within the body in other organs and (connective) tissue. Due to their significance, they present an interesting prospect as far as diagnosis and treatment of defects, especially structural, that would occur in these tissues and organs. The AFM, with its ability to be applied at ever lower dimensions opens up even greater possibilities for the nano-characterization of the collagens.

The next step in such investigations might involve the fabrication of devices based on the AFM to enable even earlier detection of degenarative defects leading to better management of those that have no cure yet like OA. Better yet, deeper understanding of the workings and properties of the collagens from investigations with the AFM coupled with other methods might be the beginnings of the development of synthetic polymers that could be used in regenerative therapies so be a cure for these defects.

REFERENCES

Adachi E. *et al*. Collagen II containing a Cys substitution for Arg-α1-519. Analysis by atomic force microscopy demonstrates that mutated monomers alter the topography of the surface of collagen II fibrils, *Matrix Biology*, 18, 189-196, 1999.

Bozec L, Horton M. Topography and mechanical properties of single molecules of type I collagen using atomic force microscopy. *Biophysical Journal*, 88, 4223-4231, 2005.

Brodsky, B., Eikenberry, E. F., Characterization of fibrous forms of collagen, *Methods Enzymol*., 82, 127-74, 1982.

Broom, N.D., Marra, D.L., Ultrastructural evidence for fibril-to-fibril associations in articular cartilage and their functional implication. *Journal of Anatomy,* 146, 185–200. 1986.

Buehler, M., Nature designs tough collagen: Explaining the nanostructure of collagen fibrils, *PNAS*, 103, 12285-12290, 2006.

Buehler, M.J., Atomistic and continuum modeling of mechanical properties of collagen: Elasticity, fracture, and self-assembly, J. *Mater. Res.,* 21, 8, 1947-1961, 2006.

Bustamante, C., J. F. Marko, E. D. Siggia, and S. Smith. Entropic elasticity of λ-phage DNA. *Science*, 265, 1599–1600, 1994.

Cisneros, D. A., Hung, C., Franz, C. M. & Muller, D. J. Observing growth steps of collagen self-assem- bly by time-lapse high-resolution atomic force micro- scopy. *J. Struct. Biol.* 154, 232–245, 2006.

Dudko OK, Hummer G, Szabo A. Theory, analysis, and interpretation of single-molecule force spectroscopy experiments. *Proceedings of the National Academy of Sciences of the United States of America*, 105, 15755-15760, 2008.

Evans, E., and Ritchie, K. Dynamic strength of molecular adhesion bonds. *Biophysical Journal*, 72, 1541–1555, 1997.

Fertala, A., Sieron, A.L. et al., Self-assembly into Fibrils of Collagen II by Enzymic Cleavage of Recombinant Procollagen II, Journal of Biological Chemistry, 269, 15, 11584-11589, 1994.

Friedrichs J, Taubenberger A, Franz CM, Muller DJ. Cellular remodelling of individual collagen fibrils visualized by time-lapse AFM. *Journal of molecular biology*, 372, 294-607, 2007.

Gelse K. Collagens—structure, function, and biosynthesis. *Advanced Drug Delivery Reviews*, 55, 1531-1546, 2003.

Graham, J.S. Mechanical Properties of Complex Biological Systems using AFM-Based Force Spectroscopy. *PhD thesis,* University of Missouri-Columbia, 2005.

Gutsmann T, Fantner GE, Kindt JH, et al. Force spectroscopy of collagen fibers to investigate their mechanical properties and structural organization. *Biophysical journal*, 86, 3186-93, 2004.

Janshoff, A. et al, Force Spectroscopy of Molecular Systems-Single Molecule Spectroscopy of polymers and Biomolecules, *Angew. Chem. Int. Ed.*, 39, 3212-3237, 2000.

Jiang F, Hörber H, Howard J, Müller DJ. Assembly of collagen into microribbons: effects of pH and electrolytes. *J. Struct. Biol.* 148, 268-278, 2004.

Kaab, M.J., Gwynn, I.A., Notzli, H.P., Collagen fibre arrangement in the tibial plateau articular cartilage of man and other mammalian species. *Journal of Anatomy*, 193 23–34, 1998.

Kuo, S. M. et al, Influence of Alginate on Type II collagen fibrillogenesis, Journal of Material Science: Material Science in Medicine, 16, 525-531, 2005.

Lin, H. et al, Imaging Real timeProteolysis of Single Collagen I Molecules with an Atomic force microscope, *Biochemistry,* 38, 9956-9963, 1999.

Minns, R.J., Steven, F.S., The collagen fibril organization in human articular cartilage. *Journal of Anatomy*, 123, 437–457, 1977

Morris VJ, Kirby AR, Gunning AP. Atomic Force Microscopy for Biologists. Imperial College Press, London. 2010

Neuman KC, Nagy A. Single-molecule force spectroscopy: optical tweezers, magnetic tweezers and atomic force microscopy. *Nature Methods*, 5, 491-505, 2008.

Pieper, J.S. et al., Preparation and characterization of porous crosslinked collagenous matrices containing bioavailable chondroitin sulphate, *Biomaterials*, 20, 847-58, 1999.

Piepera, J.S. et al., Crosslinked type II collagen matrices: preparation, characterization, and potential for cartilage engineering, *Biomaterials*, 23, 3183–3192, 2002

Ricci D, Braga PC. Atomic Force Microscopy Biomedical Methods and Applications. *Methods in Molecular Biology*. 2004; 242.

Rich, A., Crick, F. H. C. The Structure of Collagen. *Nature*, 176, 915-916, 1955.

Santos NC, Castanho M a RB. An overview of the biophysical applications of atomic force microscopy. *Biophysical chemistry*, 107, 133-49, 2004.

Shapiro AL, Vinuela E, Maizel JV Jr. Molecular weight estimation of polypeptide chains by electrophoresis in SDS-polyacrylamide gels, *Biochem Biophys Res Commun.* 28 815–820, 1967.

Shirazi R, Shirazi-Adl A, Hurtig M. Role of cartilage collagen fibrils networks in knee joint biomechanics under compression. *Journal of biomechanics*, 41, 3340-8, 2008.

Stolz M, Gottardi R, Raiteri R, et al. Early detection of aging cartilage and osteoarthritis in mice and patient samples using atomic force microscopy. *Nature Nanotechnology*, 4, 186 – 192, 2009.

Stolz M, Raiteri R, Daniels a U, et al. Dynamic elastic modulus of porcine articular cartilage determined at two different levels of tissue organization by indentation-type atomic force microscopy. *Biophysical journal*, 86, 3269-83, 2004.

Stolz, M., et al. Dynamic elastic modulus of porcine articular cartilage, *BioWorld*, 4, 2-5, 2003.

Sun HB, Smith GN, Hasty K a, Yokota H. Atomic force microscopy-based detection of binding and cleavage site of matrix metalloproteinase on individual type II collagen helices. *Analytical biochemistry*. 283, 153-8, 2000.

Sun Y-L, Luo Z-P, Fertala A, An K-N. Stretching Type II Collagen with Optical Tweezers. *Journal of biomechanics*, 37,1665-9, 2004.

Temple MM, Bae WC, Chen MQ, et al. Age and site-associated biomechanical weakening of human articular cartilage of the femoral condyle. *Osteoarthritis and cartilage / OARS, Osteoarthritis Research Society*. 15, 1042-52, 2007.

Yang L. Mechanical properties of collagen fibrils and elastic fibers explored by AFM, *PhD Thesis*, University of Twente, 2008.

Zlatanova J, Lindsay SM, Leuba SH. Single molecule force spectroscopy in biology using the atomic force microscope. *Progress in biophysics and molecular biology*, 74, 37-61, 2000.